

Irradiated sodium-alginate/poly(ethylene oxide) blend films improved by methyl acrylate monomer

Sumaia Aktar Sumi,¹ Wasikur Rahman,^{1,2} Jahangir Alam,¹ Nirmal Chandra Dafader,³ Serajum Manir,³ Maksudur Rahman Khan²

¹Department of Chemical Engineering, Jessore University of Science and Technology, Jessore 7408, Bangladesh

²Faculty of Chemical and Natural Resources Engineering, Universiti Malaysia Pahang, 26300 Gambang, Kuantan, Malaysia

³Nuclear and Radiation Chemistry Division, Institute of Nuclear Science and Technology, Bangladesh Atomic Energy Commission, Dhaka 1207, Bangladesh

Correspondence to: M. W. Rahman (E-mail: mw.rahman@just.edu.bd or mwrahman.ump@gmail.com)

ABSTRACT: Sodium alginate (SA)-based poly(ethylene oxide) (PEO) blend films were improved by methyl acrylate (MA) monomer and γ irradiation toward practical application. The films were prepared by a casting method and modified by glycerol (Gol) and mustard oil (MO). The SA-based films were successfully produced with γ irradiation (12 kGy) with 10% PEO, 15% Gol, 20% MO, and 7% MA on a mass basis as optimized. The tensile strength (TS), tear strength (TT), elongation at break (EB), Young's modulus, moisture content, water vapor permeability (WVP), and structural properties of the blended films were determined. The thermal properties of the films were characterized by thermogravimetric analysis, dynamic mechanical analysis, and differential scanning calorimetry, and the structural features were examined with Fourier transform infrared spectroscopy. The ultimate results of this study show a rather remarkable enhancement in the tensile properties (30% TS and 67% TT) and reduction in EB (40%) of the SA-based films with MA addition and γ irradiation. The as-prepared SA-based films demonstrated considerable reductions in the moisture content and WVP and also conferred a desired stability of the films. © 2016 Wiley Periodicals, Inc. *J. Appl. Polym. Sci.* **2016**, *133*, 43562.

KEYWORDS: differential scanning calorimetry (DSC); grafting; irradiation; mechanical properties; packaging

Received 7 October 2015; accepted 19 February 2016

DOI: 10.1002/app.43562

INTRODUCTION

To meet the present demand for polymeric materials with desired properties, cost effectiveness, and ease of processing, the importance of polymeric blends is gradually increasing. Polymeric blends are mixtures of various polymers or copolymers that interact without covalent bonding, such as dipole–dipole forces, hydrogen bonding, or charge–transfer complexes.^{1–4} The blend materials still suffer from drawbacks in meeting all of the complex demands of the biomaterials. Synthetic polymers show high mechanical properties, transformation processes, and low production costs but a poor biodegradability. On the contrary, natural polymers present good biocompatibility, but their mechanical properties are not satisfactory. The challenge of preserving the biological properties of the materials is a current issue; however, they show adverse effects on complex processing and a high production or recovery cost. Therefore, the blending of polymeric materials based on synthetic and natural polymers is a challenge.⁵

To overcome the challenges of preparing biodegradable polymeric materials and to achieve the desired properties of biopolymers,

the advance modification of sodium alginate (SA)-based films has been achieved through monomer addition and γ irradiation.^{6,7} The effects of α irradiation on molecular bonding and polymer structures are very crucial, as studied by Wood and Pikaev.⁸ A number of routes have been explored to improve the mechanical properties of natural polymer films; these include grafting with electromagnetic radiation, such as γ rays and UV light, and free-radical initiators. In the last decade, the application of α radiation has emerged as a vital tool in the development of polymerization techniques.^{9,10} The use of α radiation offers many advantages over the use of UV radiation¹¹; these advantages include continuous operation, a minimum time requirement, and design flexibility. Moreover, environmental pollution due to α irradiation is comparable to that produced by chemical methods.¹² On the contrary, radiation can be applied for polymer degradation (e.g., degradation of pectin, alginate, milk protein, gelatin, chitosan) to produce low-molecular-weight substances^{13–15} and to form film-forming materials.^{16,17}

The state-of-the-art technology of biofilm formation through blending is to date an unresolved issue. In fact, the modification

of SA-based films with poly(ethylene oxide) (PEO) followed by the addition of monomers to the blends for grafting is a widespread technology.^{18–21} SA, being a polyelectrolyte, has a rigid molecular chain¹⁸ and good film-forming ability, whereas PEO is a unique class of water-soluble, aerobically biodegradable thermoplastics.¹⁹ The grafting of methyl acrylate (MA) onto partially carboxymethylated SA is quite promising, as reported in the literature.^{6,20,21} The uniform distribution of monomers in polymer suspensions is very essential for proper grafting.²² Therefore, SA–PEO blends need to be tailored by plasticizers [e.g., glycerol (Gol)] and emulsifiers [e.g., mustard oil (MO)] before monomer (MA) addition. MO can stabilize biopolymer dispersion results with increasing moisture resistance of the films.²³ To the best of our knowledge, SA–PEO blends including Gol, MO, and MA grafted by γ irradiation have not been studied in detail so far from a practical point of view.

The ultimate goal of this study was to develop biodegradable polymeric materials, particularly, to improve SA–PEO blend films by the addition of MA monomer and α irradiation, particularly with respect to their mechanical properties, water-barrier properties, thermal stability, and structural features. All of the film-forming additives and radiation doses were optimized as well.

EXPERIMENTAL

Materials

SA (molecular weight \approx 200,000 g/mol, Unichem, India), PEO (molecular weight \approx 300,000 g/mol, Sigma–Aldrich, United States), Gol and methanol (Merck, Germany), MA (Fluka Chemica, Switzerland), and MO (from a local market) were collected for the experiment and were used as received.

Preparation of Pure SA Films

We prepared an aqueous solution of SA (2.5 wt %) by stirring 2.5 g of SA and 97.5 mL of water for at least 2–3 h until the mixture became homogeneous. Then, we kept the solution at rest for 1 h to remove bubbles by settling it at room temperature; we then poured the aqueous solution onto a glass plate to prepare thin films. The films were dried at 60 °C in an oven *in vacuo* until they turned transparent. Finally, the dried films were stored for characterization.

Preparation of the PEO Solution

We prepared an aqueous solution of PEO (2.5 wt %) by pouring 97.5 mL of water into 2.5 g of PEO and shaking the mixture continuously to prevent agglomeration. Then, the mixture was placed in an autoclave at 250 °C under 15 psia of pressure for about 1 h. The solution afterward was taken out of the autoclave, placed in open air to achieve room temperature, and finally applied for further preparation.

Preparation of the SA–PEO Blend Films

SA and PEO blend was prepared by the mixture of a formerly prepared 2.5 wt % aqueous solution of both SA and PEO under different compositions (0, 5, 10, 20, 30, and 40 wt % PEO and balance SA). The films were prepared with the same method applied for the pure alginate films. Then, the films were characterized to optimize the composition of the blends. The best tensile properties were found in the SA–PEO 9:1 w/w blend film, which was considered in further experiments.

Preparation of the SA–PEO–Gol Blend Films

An SA–PEO–Gol blend was prepared with a previously optimized SA–PEO 9:1 w/w film and Gol with various compositions (0, 10, 15, 20, 25, and 30 wt %). The method applied for the preparation of the pure SA films was also followed for this case. Then, the tensile properties of the films were studied to optimize its composition, and we found the best results with 15 wt % Gol. So, further work was done with the blend with a composition of SA–PEO 9:1 w/w and 15 wt % Gol.

Preparation of the SA–PEO–Gol–MO Blend Films

The SA–PEO–Gol–MO blend was prepared by the earlier optimized SA–PEO 9:1 w/w and 15 wt % Gol and MO of various compositions (0, 10, 15, 20, 25, and 30 wt %). The same method was followed to make polymer films as described previously. Then, we characterized the films by optimization of their compositions in the blend and found best the properties for 20 wt % MO. So, the films with the blend composition SA–PEO 9:1 w/w and 15 wt % Gol and 20 wt % MO were considered in the next experiment.

Modification of the SA–PEO Films with MA

The SA–PEO formulated films were modified further with MA monomer and γ irradiation. The previously prepared blend (SA–PEO 9:1 w/w, 15 wt % Gol, and 20 wt % MO) were soaked in four different formulations of MA (0, 3, 5, 7, 10, and 15 wt %, and 1:1 v/v balance methanol–water solution). The casting method was followed to make the SA-based films, and the films were characterized to optimize the composition in the blend. The best results were obtained for 7 wt % MA as optimized. Therefore, the films with the blend composition with SA–PEO 9:1 w/w, 15 wt % Gol, 20 wt % MO, and 7 wt % MA was considered for γ irradiation.

Modification of the SA-Based Films with γ -Irradiation

The SA–PEO blends incorporated with Gol, MO, and MA were treated with α irradiation from a ⁶⁰Co source at a dose rate of 2.5 kGy/h in the presence of oxygen. The dose rate was determined with the help of a Fricke dosimeter. The blends were irradiated with various doses (0, 3, 5, 7, 10, 12, 15, and 20 kGy) for optimization. The blends with different additives are represented in this article by the capitalized first letters of each additive: SP for SA and PEO; SPG for SA, PEO, and Gol; SPGM for SA, PEO, Gol, and MO; and SPGMM for SA, PEO, Gol, MO, and MA.

Tensile Property Measurement. The tensile properties of the films were measured by Testometric Rochdale England (DBBMTCL-250 kg) with a crosshead speed of 2 mm/min. A load range of 500 N and a gauge length of 20 mm were used throughout the experiment. To evaluate the tensile strength (TS) and tear strength (TT), the ISO 37-1977(E) and ISO 34-1975(E) methods, respectively, were followed.

Moisture Absorption Measurement. The films were cut into a 0.5-cm size. Then, they were dried in an oven and weighed successively at 1-h intervals until the weight became approximately constant. These films were kept at a temperature of 298 K and a relative humidity of 78% to measure moisture absorption and

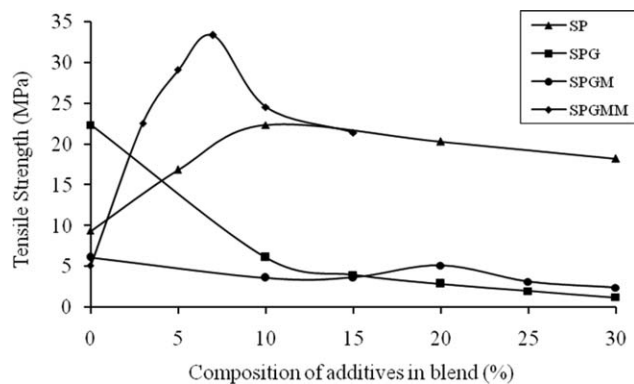


Figure 1. TS values of SA-based films modified with various additives (PEO, Gol, MO, and MA). The SPGMM blend contained 10 wt % PEO, 15 wt % Gol, 20 wt % MO, and a variable amount of MA. MO, Gol, and PEO were variable additives in the SPGM, SPG, and SP blends, respectively, for optimization.

weighed as earlier at 1-h intervals. Then, the moisture absorption was calculated by the following equation:

$$\text{Moisture absorption (\%)} = [(W_m - W_d) / W_d] \times 100$$

where W_m is the weight of the moisture absorbed and W_d is the weight of the dry films.

Procedure for Determining the Water Vapor Permeability (WVP). Circular WVP cups made from Perspex were manufactured according to the specifications reported by McHugh *et al.*²⁴ Briefly, distilled water (6 mL) was placed in each test cup, and a film sample was mounted across the cup opening. The cups were stored under controlled temperature (298 K) and relative humidity (78%). A constant air velocity of 152 m/min was maintained over the cups to ensure uniform air movement across the WVP test cells. Steady-state conditions were reached within 2 h. The weight losses of the cups were monitored over a 24-h period, with the weights recorded at 2-h intervals. WVP was calculated according to the protocol specifications, which were a modification of the ASTM E-96 standard method²⁵ for determining WVP ($\text{g mm kPa}^{-1} \text{d}^{-1} \text{m}^{-2}$) of synthetic packaging materials:

$$\text{WVP} = m \times L / A \times T \times \Delta p$$

where m is the weight of water permeated through the film, L is the thickness of the film, A is the permeation area of the film (22.62 cm^2), T is the permeation time, and Δp is the difference between the water vapor pressures on both sides of the film.

Thermogravimetric Analysis (TGA)

Dynamic weight loss tests were conducted with a thermogravimetric analyzer (PerkinElmer TGA 7). All tests were accomplished in a continuous N_2 purge (20 mL/min) over the temperature range 30–500 °C at a scanning rate of 10 °C/min.

Differential Scanning Calorimetry (DSC)

The thermal stability of the films was obtained by DSC measurements (DSC-60, 230 v, Shimadzu Co., Japan, equipped with a thermal analyzer, T_A-60 WS) in the temperature range 30–500 °C at a heating rate of 10 °C/min under an N_2 atmosphere

(flow rate = 200 mL/min). Samples with an average weight of 2 mg were placed in the DSC chamber for each run.

Dynamic Mechanical Analysis (DMA)

The thermal properties of the films were studied by means of DMA (Triton Technology TTDMA, United Kingdom) from 28 to 200 °C at a heating rate of 4 °C/min and an oscillating frequency of 1 Hz.

Fourier Transform Infrared (FTIR) Spectroscopy

The structural information of the formulated films and pure precursor materials was attained by an FTIR spectrometer (Imprestige 21, Shimadzu Co., Japan) equipped with an attenuated total reflectance device in the wave-number range 500–4000 cm^{-1} at a scanning rate of 20 °C/min and a resolution 4 cm^{-1} . The FTIR spectra were taken in a transmittance mode.

RESULTS AND DISCUSSION

Effect of the Additives on the SA-Based Films

The tensile properties of various SA-based films are shown in Figures 1–3. The TS, elongation at break (EB), and Young's modulus (YM) values of the SP, SPG, SPGM, and SPGMM blend films were examined. The effect of the radiation doses on the formulated films were predominant; nevertheless, the consequences of the monomer (MA) and PEO in the blends were clear. Moreover, the addition of plasticizer (Gol) and emulsifier (MO) affected the tensile properties significantly. In general, PEO and MA improved TS and YM but reduced EB, whereas Gol and MO showed the reverse activities on the films. The compositions of the additives in the blends showed strong effects on the tensile properties of the films and were optimized.

Effect of PEO on the SP-Based films

The effects of PEO on the TS, EB, and YM values of the SP blend films (\blacktriangle) is shown in Figures 1–3, respectively. PEO increased TS and YM but decreased EB. With increasing concentration of PEO in the blend, TS and YM increased up to 139 and 55.84%, respectively, for 10 wt % PEO and then started to decrease (Figures 1 and 3). Under the same conditions, EB decreased up to 54.30% and then slightly increased (Figure 2).

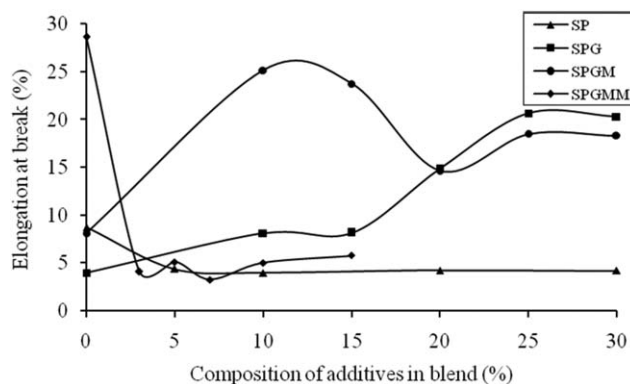


Figure 2. EB values of SA-based films modified with various additives (PEO, Gol, MO, and MA). The SPGMM blend contained 10 wt % PEO, 15 wt % Gol, 20 wt % MO, and variable amounts of MA. MO, Gol, and PEO were variable additives in the SPGM, SPG, and SP blends, respectively, for optimization.

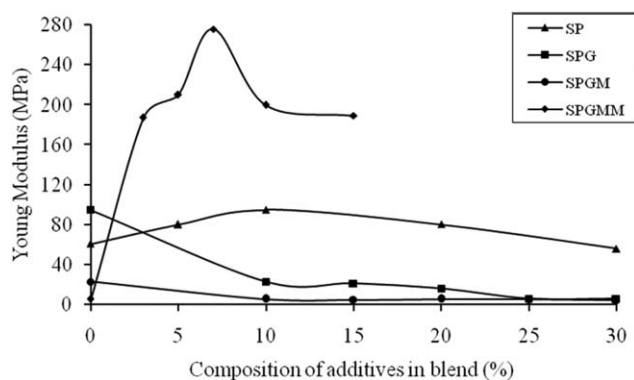


Figure 3. YM values of SA-based films modified with various additives (PEO, Gol, MO, and MA). The SPGMM blend contained 10 wt % PEO, 15 wt % Gol, 20 wt % MO, and variable amounts of MA. MO, Gol, and PEO were variable additives in the SPGM, SPG, and SP blends, respectively, for optimization.

As a result, 10 wt % PEO was considered as an optimum value for the SA–PEO 9:1 w/w blend. During the modification of SA with PEO, they combined together by intermolecular hydrogen bonding between the hydroxyl groups (—OH) of SA and oxygen atoms of PEO.²⁶ Similar results were also reported for blend films of silk fibroin/SA²⁷ and polyacrylamide/SA.²⁸ Therefore, TS and YM increased more than those of the pure alginate films, and EB decreased as well. Nevertheless, with more than 10 wt % PEO, the tensile properties showed overturned effects because of the fact that at a higher concentration of PEO, a denser network structure was formed; this restricted the mobility of the molecules. As a result, TS and YM decreased, and EB increased.²⁹

Effect of Gol on SPG Films

Figures 1–3 show that with increasing concentration of Gol in the SPG blend (■), TS and YM decreased, but EB increased up to a 15 wt % concentration, which was regarded as the optimum value. With further increases in the concentration of Gol, the SPG films showed adverse effects on the mechanical properties. Gol, as a plasticizer, was added to the blends and improved the flexibility of the films; alginate–PEO films plasticized with Gol showed better water permeability and flexibility as they exhibited higher deformations and elongations than the SA–PEO blend. The water permeability of the SP blend films increased with increasing Gol contents; this may have been due to decreasing intermolecular attractions and increasing molecular mobility in the film matrix, which resulted from the addition of Gol molecules between polymer chains. The increased mobility resulted in a greater free volume in the matrix; this facilitated the migration of water molecules through the films.^{20,30,31} The high hydrophilicity of Gol molecules, which was favorable to the adsorption of water molecules, could also contribute to the increase in the film's water permeability.²⁹ Additionally, at a high Gol concentration, Gol could cluster with itself to open polymer structures; this enhanced the permeability of the film to moisture.³² Moreover, the addition of Gol (>33.3%, dry basis) resulted in sticky, wet films. The concentrations of Gol needed for forming blend films fell into the range 15–60 wt %, the same used for forming other biopolymer films,

depending on the properties of the polymers and the purpose of their applications.^{21,29,33} Further modification was done with monomer grafting to improve the mechanical properties of the films.

Effect of MO on the SPGM Films

To improve flexibility and homogeneity in the SPGM blend (•), MO was used as an emulsifier. We found that the incorporation of MO of up to 20 wt % in the blend further decreased TS and YM (Figures 1 and 3) and increased EB (Figure 2). In addition, MO altered the properties of the base polymer (SP blend) in the same manner. So, 20 wt % MO was selected for further processing.

Effect of MA on the SPGMM Films

The SPGM blend (◆) was mixed with MA monomer with different compositions (0, 3, 5, 7, 10, and 15 wt %), and we characterized the mechanical properties of the films to optimize them by monomer addition. The TS, EB, and YM values of the blend films as a function of the blend composition are presented in Figures 1–3. TS and YM were found to increase with increasing concentration of MA; they reached maximum values for 7 wt % MA. In contrast, EB gradually decreased up to the value as optimized. The tensile properties of the SPGMM films varied when equipped with 15 wt % MA.

Effect of the Radiation Doses on the SPGMM Films

As the best tensile properties were obtained for 7 wt % MA, the TS, TT, and EB values of the SPGMM irradiated films were studied as a function of the radiation dose for 7 wt % MA. The TS (◆), TT (▲), and EB (•) values of the irradiated films as a function of the radiation dose (0, 3, 5, 7, 10, 12, 15, and 20 kGy) are shown in Figure 4. TS and TT increased with increasing radiation dose and reached maxima of 43.38 MPa and 61.89 N/mm for a 12-kGy radiation dose. When the radiation dose was greater than 12 kGy, the values of the SPGMM films decreased. Moreover, the radiation dose increased the tensile properties of the SPGMM films by about 30% compared to those of the nonirradiated films. We expected that with the

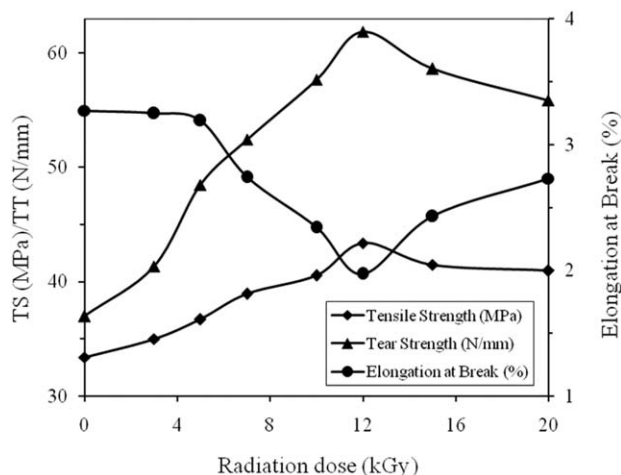
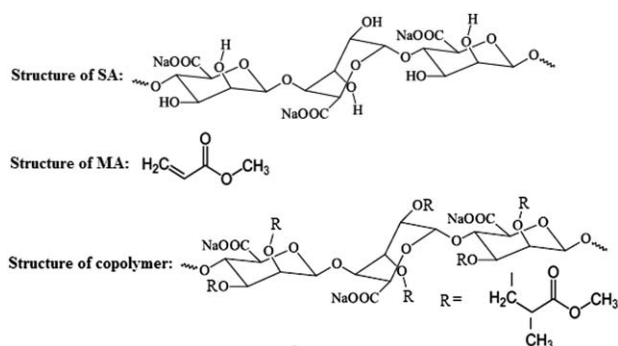


Figure 4. TS, TT, and EB values versus the radiation doses (0–18 kGy) of SA-based films modified with various additives (10 wt % PEO, 15 wt % Gol, 20 wt % MO, and 7 wt % MA).



Scheme 1. Mechanism of the grafting of MA onto SA by γ irradiation induced grafting.

increase in radiation dose, some radicals were generated in SA. These radicals may have reacted with MA to form a copolymer of alginate and MA. As a result, the TS and TT increased. Moreover, radicals could also form from MA; this promoted homopolymerization. At higher radiation doses (>12 kGy), homopolymer formation was dominant, and this suppressed the reaction between SA and MA. Higher radiation doses also caused the degradation of the polymers.^{10,34,35} Thus, at higher radiation doses, the film became hard and brittle, and TS and TT decreased. On the contrary, EB of the films decreased with increasing radiation dose up to the optimum value and then slightly decreased. At radiation doses higher than 12 kGy, EB values increased; this might have been due to the fact that after γ irradiation, the treatment rigidity of the films increased, and this caused a decrease in EB. At the optimum radiation dose (12 kGy), the films became less flexible and gained a minimum EB (39.76%); this might have been due to the maximum interaction between the polymers.

The effect of MA monomer addition to the blend was already explained by the tensile property studies (Figures 1–3); however, the properties were further examined with respect to the radiation dose. At a low monomer concentration, the monomer–polymer backbone reaction occurred (as shown in Scheme 1). Tuhin *et al.*³⁴ also reported the reaction mechanism of chitosan–starch films with 2-hydroxyethyl methacrylate. As the monomer concentration increased up to 7 wt %, more MA reacted with SA to give an extended carbon chain, and the tensile properties increased. In this situation, both the copolymerization and homopolymerization could increase. At a higher concentration of MA (>7 wt %), because of the dominant recombination process, this could create homopolymer rather than a monomer–polymer backbone reaction.^{36,37} As a result, TS decreased:

Initiation:

SA (γ radiation) \rightarrow SA $^{\circ}$ (primary free radical)

SA $^{\circ}$ + MA \rightarrow SA–MA $^{\circ}$ (chain free radical)

Propagation:

SA–MA $^{\circ}$ + n MA \rightarrow SA–MA $_{n+1}$ $^{\circ}$ (graft growing chain)

Termination:

SA–MA $_{n+1}$ $^{\circ}$ + CH₃OH \rightarrow SA–MA $_{n+1}$ (graft copolymer)

where n defines number of moles of MA monomer reacted in the polymerization reaction, SA stands for sodium alginate and MA stands for methyl acrylate.

Effect of the Moisture Absorption and WVP on the SPGMM Films

The moisture absorption capacity and WVP of the SPGM, SPGMM, and irradiated SPGMM films at 12 kGy were studied for a 24-h immersion period, and the results are shown in Figure 5. All of the samples showed two peaks: one with a shorter contact/immersion period (ca. 1 h, less intense) and the other with a longer period (16–24 h), which demonstrated the maximum absorption capacity. We observed that the SPGM films showed a lower moisture absorption capacity (10.22%) than both SPGMM (24.50%) and the irradiated SPGMM (18.20%) films for 24 h, and the WVP showed almost similar trends. In contrast, the fact that the response to WVP of the SA-based films was faster than the moisture absorption may have been due to the effect of forced convection during the rather complicated WVP experiment over the natural convection mode. The addition of MO may have reduced the hydrophilicity, moisture absorption capacity, and WVP of the films. The water-uptake values of the irradiated SPGMM films were slightly higher than those of the SPGM films but were still lower than those of the SPGMM films. This may have been due to the strong affinity of the MA monomer to water. The hydrophilic nature of MA decreased the hydrogen bonds between the polymer chains, and this resulted in a greater intermolecular space and increased the permeability of the film to moisture and oxygen. So, after the addition of MA, the moisture absorption increased for the SPGMM films. However, the radiation reduced the absorption capacity of the films. When the films were modified with MA and radiation, the moisture/vapor content values were lower because monomer grafting (copolymerization) occurred, and this strongly reduced the permeability of the film to water.³⁴ An interesting approach to reduce WVP values is to develop multilayer or laminate films; this resembles the production of multilayer synthetic packaging films.^{38,39} In addition, the particle size, molecular weight, pH, nature of the ions,

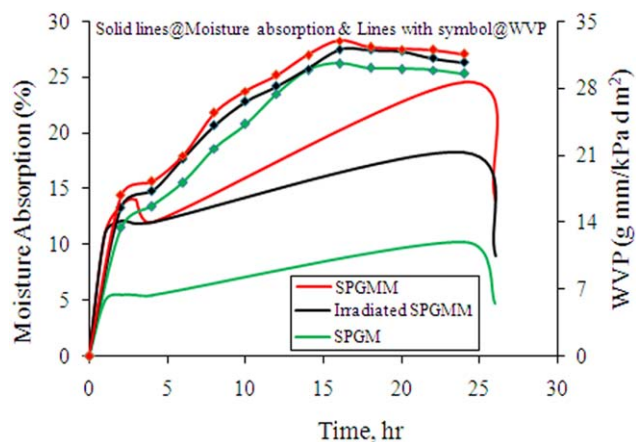


Figure 5. Rates of moisture absorption and WVP values of SPGM, SPGMM, and irradiated SPGMM films. [Color figure can be viewed in the online issue, which is available at wileyonlinelibrary.com.]

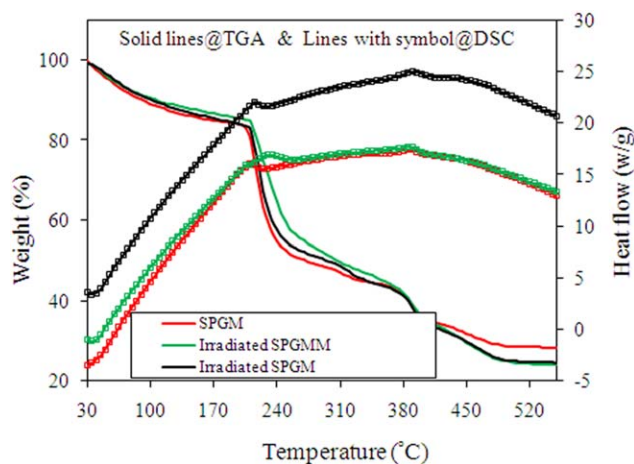


Figure 6. TGA plots of the weight and DSC curves of the heat flow versus temperature for the SPGM, irradiated SPGM, and irradiated SPGMM films. [Color figure can be viewed in the online issue, which is available at wileyonlinelibrary.com.]

ionic strength, and so on are the key factors in moisture uptake into the polymer structure.^{22,40} A reduced particle size may increase the moisture-barrier properties of a biopolymer film because of the creation of tortuous pathways by which water molecules are transported through the film.⁴¹ Mollah *et al.*⁴⁰ reported that SA-based films could be broken down into smaller molecules during α irradiation, and reduced absorption capacity resulted as well. Thus, modified films showed improved water stability. It was also observed that the water-uptake values of the films started to decrease with increasing immersion time; this might have been due to the degradation of the swollen films.

TGA

The TGA thermograms of the formulated SPGM, irradiated SPGM, and irradiated SPGMM films are shown in Figure 6 to clarify the effects of the monomer addition and radiation dose. We observed that the thermal stability of the SPGM films was improved by radiation and further improved by MA monomer addition. The thermograms of the films showed weight losses mainly in three regions: 30–210, 210–250, and 250–390 °C. The total weight loss of the SPGM films without radiation from 30 to 210 °C was found to be 10.75 wt % in the first step, whereas the weight losses of the films with radiation (12 kGy) and irradiated films with monomer (MA) in this range were found to be 9.74 and 9.40%, respectively. This was due to the loss of absorbed or residual moisture.^{6,34,42} The second-stage weight loss was referred to as the pyrolysis step. These three films showed sharp weight losses (~40%) in the temperature range 210–250 °C; this was due to the residual ungrafted SA. Caykara *et al.*²⁶ reported that the weight loss of pure SA occurred in the temperature range 229–243 °C. The degradation of the grafted copolymer probably occurred in the third step (250–390 °C). The weight loss of the pure PEO began at 360 °C and continued up to 395 °C. Moreover, the initial thermal degradation temperatures of the blends may have been affected by SA, PEO, Gol, MO, and the MA monomer, as reported earlier for SA–PEO. At higher temperatures (>390 °C), weight loss occurred because of

carbonization. It was also evident from the TGA curve that a 50% weight loss of the grafted copolymer was detected at 305 °C; this temperature was higher than that for ungrafted polymer (270 °C).

The gradual thermal degradation of pure SA was examined by Yang and Chiu;⁴³ they found that there were two stages of thermal degradation. The first stage was due to the elimination of side groups at about 240–300 °C, and the second stage occurred at about 620–670 °C (this was not found in our case because of instrumental restriction). The second stage was due to the breakdown of the polysaccharide backbone of SA. Except for the elimination of water molecules at about 50–150 °C, two stages of thermal degradation were also found for pure poly(vinyl alcohol) (PVA). The first and the second stages were due to the elimination of side groups at about 290–460 °C and the breakdown of the polymer backbone of PVA at about 500–570 °C. Finally, the dual effects of the monomer and radiation dose on the SA-based films were tested quite successfully through examination of the thermal stability of the films, even far beyond the normal temperature.

DSC Analysis

Figure 6 shows the three DSC curves of SPGM, irradiated SPGM, and MA-integrated irradiated SPGMM films to illustrate the effect of the monomer on thermal stability. All of the curves exhibited particular endothermic peaks around 30–40 °C; this was followed by second and third exothermic peaks located at 203–234 and 377–396 °C, respectively. It has been reported that the detected endothermic and exothermic peaks corresponded to dehydration and decomposition, respectively.^{44,45} The second and third exothermic peaks corresponded to the decomposition of SA at 229–243 °C and that of PEO at 360–395 °C, as illustrated earlier by TGA. Moreover, the SA–PEO blends degraded in two distinct steps around 240 and 408 °C.²⁶ Yang and Chiu⁴³ reported that the melting point of SA–PVA films decreased with increasing SA content in the films. In addition, a polymer with a higher crystallinity had a higher melting point and a higher heat of fusion.⁴³ The crystallinity in the SA–PEO films decreased with increasing content of SA in the films. Because of the conformation of the amorphous chain of SA in the PVA–SA membrane, the crystalline area of the PVA–SA membrane was destroyed in comparison with that of the pure PVA.⁷ As a result, the melting point of PEO in the SA–PEO blend films might have decreased (240 °C) from that of the pure form (360 °C). The DSC curves did not display any peak attributed to the intermediate additives (Gol and MO). This suggested that their effect was insignificant; probably because of the low molecular weight of the conjugated molecules, which limited their influence on the polymer properties.⁴⁵ These results were in agreement with those obtained from TGA, where dehydration was observed at temperatures up to 210 °C. Furthermore, the first decomposition step was detected around 250 °C for all of the samples. Similar results were also reported by Pinhas and Peled.⁴⁵

The thermal characteristics of the pure SA, PEO, and their blends are available in the literature.^{6,7,16,26,45} The endothermic peaks in our case were obtained at 30–40 °C, whereas in

previous investigations, they were detected at around 60 °C,^{26,45} 59 °C,⁴⁶ 67 °C,⁴⁷ and 55 °C,⁴⁸ depending on the details of the experimental protocol (heating rate, type of gas used, gas flow rate, etc.).⁴⁴ In addition, we obtained two exothermic peaks at 203–234 and 377–396 °C; these values corresponded with those reported in published articles. Similar characteristic peaks at 260 °C⁴⁷ and 256 °C⁴² were detected for the alginate films. However, the peaks detected at higher temperatures (377–396 °C) have rarely been explained in the literature and may have been due to the decomposition of the SA-based polymer backbone of the films, as elucidated by TGA.⁷ The fact that these values were little higher than our findings may have been due to the effects of the plasticizer (Gol) and emulsifier (MO) addition. A comparison of the thermograms obtained for the SA-based conjugation blend suggests that PEO–MA grafting retained the characteristic decomposition of alginate. The intensity of the peaks was reduced because of the lower alginate mass ratio in the sample; this was a consequence of the high molecular weight of PEO (molecular weight \approx 300,000 g/mol).⁴⁰

In addition, the characteristic melting peak of the irradiated SPGMM was shifted to a higher temperature; that of irradiated SPGM shifted upward, and all of the peaks became broader. Laurienzo *et al.*⁴⁸ also detected a smaller and shifted melting peak of poly(ethylene glycol) (PEG) conjugated with alginate. The shift was attributed to the hampering of the crystallization process through the reduced mobility of the PEG chains due to the grafting reaction. Similar behavior was also detected in PEG/alginate blends.^{16,45} Moreover, the degree of crosslinking in the SA-based samples may have resulted in the temperature range with little variation, as verified by the peak broadening and the small shoulder.

In general, a good correlation was found between the results obtained by the two techniques used to analyze the thermal behavior, TGA and DSC. The previous results show that the grafting of PEO to alginate influenced its thermal behavior and increased its hydrophilicity. Nevertheless, this modification did not decrease the thermal stability at temperatures below 400 °C. Because stability tests of food-packaging materials are usually performed at temperatures of up to 100 °C, the SA–PEO–Gol–MO–MA films could be safely used from a practical viewpoint.

DMA

The glass-transition phenomena and viscoelasticity of the polymeric materials are important factors for determining the dynamic mechanical properties of the films. The glass-transition temperature (T_g) is often measured by DSC, but the DMA technique is more sensitive and yields more precise data. DMA can also be used to investigate the frequency-dependent nature of the transition. Therefore, DMA was used to explore the behavior of the alginate films in this study.

Figure 7 shows the change in the dynamic moduli of the formulated films (SPGM, irradiated SPGM, and irradiated SPGMM) with temperature. Each curve showed two distinct peaks: one at lower temperatures (centered at 45–65 °C) and the other at higher temperatures (centered at 150–165 °C; the peak corresponding to SPGM was ambiguous because of its very low intensity). Moreover, drops in the moduli were observed in all

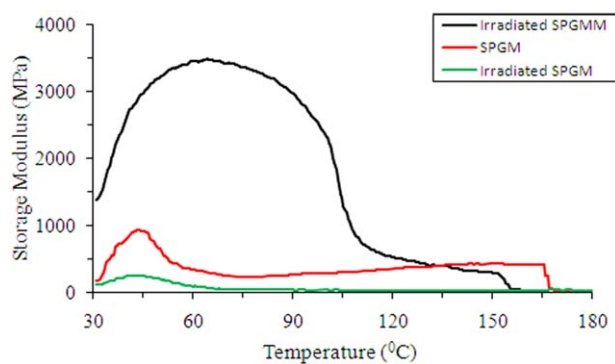


Figure 7. DMA plot of the storage modulus versus temperature for the SPGM, irradiated SPGM, and irradiated SPGMM films. [Color figure can be viewed in the online issue, which is available at wileyonlinelibrary.com.]

of the cases. The initial moduli also did not exhibit similar trends. We observed that the MA-monomer-incorporated SPGM blend films demonstrated a higher modulus than that of SPGM. The storage modulus of the irradiated SPGMM films increased up to about 65 °C and then showed a downhill trend. This transition is called the α transition, and its value, around 38 to 102 °C in this case, was defined as the glassy region. The alginate films showed two-step transitions: the first transition of the films at a lower temperature was related to its behavior changes because of water evaporation; this was followed by the second transition at a higher temperature, called T_g , at which the alginate film changed its behavior from glassy to rubbery. A sharp drop in the storage modulus was detected in the T_g region, and in this region, the behavior of alginate films moved to a leathery-state plateau region known as the noncrystalline region caused by the micro-Brownian motion.

Three relaxations may be measured by DMA but in this study only α relaxation is discussed that is, >0 °C. Relaxation in the T_g region of SA depended on water, which acted as a plasticizer. First transition of water-plasticized SA observed by the broad water desorption peaks in the vicinity of 38–102 °C. The free and physically absorbed water molecules are removed easily from the system by heating up to 120 °C.^{23,49–51} Pure SA film showed two peaks at 65 and 155 °C. Results reported elsewhere^{52,53} are analogous to this study. The first α -relaxation peak might be formed by intramolecular moisture; second one indicates T_g of SA. Caykara *et al.* showed that melting point of SA:PEO = 9:1 (w/w) blend films is 64 °C²⁶ and T_g of pure SA has been reported 158 °C.⁵² Moreover, we observed that the temperature of first α -relaxation peak for SPGM films compared to that of MA treated SPGM films was increased from 44 to 65 °C. This might be due to the presence of monomer in the blend, reduced hydrophilicity of the films.

The shift in the T_g of the irradiated SPGMM blend films at lower temperature because of the evolution of amorphous properties through distortion of crystallinity of the films studied by TGA and DSC. The composition dependent shift in T_g of the blends after the addition of hydroxyethyl cellulose followed the same trends as observed in the crystalline/amorphous portion of the polymer blends.^{54,55} With the exception of the

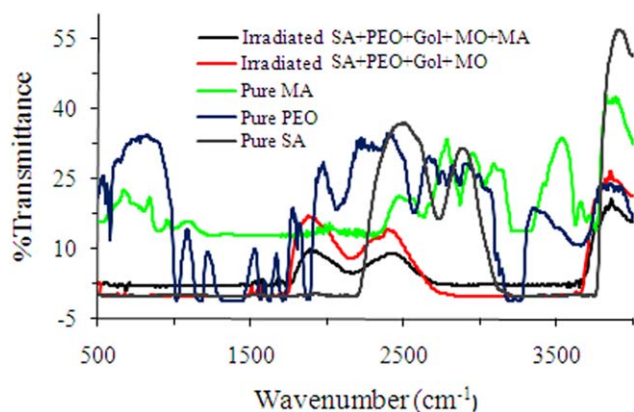


Figure 8. FTIR spectra of the transmittance versus the wave number for various SA-based films and pure precursors. [Color figure can be viewed in the online issue, which is available at wileyonlinelibrary.com.]

composition of the blends, a number of reasons were responsible for shifting the value of T_g ; these included the heating rate, working environment (e.g., under an air or N_2 atmosphere), properties of the additives (e.g., plasticizer, emulsifier), and choice of sample holders (e.g., platinum or ceramic crucible). The most important outcome of the DMA studies was that the first transition of the film increased after modification; this might be useful for food-packaging purposes.

FTIR Analysis

The FTIR spectroscopic analysis of the irradiated SPGMM and SPGM films including pure SA, PEO, and MA were performed to investigate the interaction of MA with SA (Figure 8). In a comparison of the spectra, we noted in general that some phases were depleted and some were grown up and that the intensity of the irradiated films decreased enormously. The important discrimination was observed between the irradiated films at wave numbers around 1665 and 680 cm^{-1} . The SA-MA copolymer showed an absorption band at 1665 cm^{-1} ; this was attributed to the carbonyl group (C=O) of MA. Such bands were not present in the spectrum of SPGM. Thus, the presence of an additional band in the graft copolymer provided evidence of grafting. Patel *et al.*⁶ found an absorption band at 1740 cm^{-1} for the grafting of MA onto a partially carboxymethylated SA as well. An extra peak was obtained at the low-energy end of the spectrum (fingerprint region) at 680 cm^{-1} ; this was due to $=CH_2$ functional groups and was indicative of MA (range = 1000–650 cm^{-1}) present in the sample.

The spectroscopic outcomes from pure SA showed mainly three characteristic peaks at 3896, 2893, and 2505 cm^{-1} ; these corresponded to its hydroxyl group ($-OH$), the asymmetric stretching of $COO-$, and the symmetrical stretching of $COO-$ functional groups. These peaks also existed in synthetic copolymers with a lower intensity, and subsequent peak positions shifted to 3637, 2350, and 2153 cm^{-1} .⁵⁶ FTIR analyses of pure SA and SA-PEO blends are available in the literature.^{6,16,26,54,57,58} A sharp peak was obtained around 1543 cm^{-1} ; this was due to the stretching of $-OH$ groups. In addition, the peaks of pure PEO disappeared during the polymerization of MA with SA. As shown in the figure, the intensity of the

monomer-incorporated blend showed a lower intensity, and the peaks shifted slightly; this pointed out that MA monomer took part in the reaction and the reduction of highly reactive functional groups (e.g., $-OH$, $=CH_2$).²³ Caykara *et al.*²⁶ elucidated the fact that the intensity of the hydrogen-bond band depends on the alkalinity of the proton acceptor, the acidity of the hydrogen in the proton donor, and the possibility of their close contact. As a result of hydrogen bonding, the covalent character in the donor and acceptor is weaker; hence, the energy barrier for angle deformation becomes higher. Because these experiments were carried out by means of γ irradiation and compared with pure precursors as references, the effect of the monomer on the SA-based films was obvious.

CONCLUSIONS

PEO-incorporated SA-based films were successfully prepared with an MA monomer and γ irradiation. The films were modified by the addition of a plasticizer (Gol) and an emulsifier (MO). All additives and the irradiation dose were optimized for best results. The mechanical properties, thermal stability, and structural features of the films were examined effectively. TGA and DSC studies showed strong correlations with their outcomes because PEO grafting to alginate decreased its crystallinity and melting point with increasing SA content in the films and increased its hydrophilicity. However, this modification did not decrease the thermal stability at less than 400 °C. The T_g of pure SA obtained by DMA was found to be 155 °C. FTIR studies indicated a clear grafting reaction between MA and SA. The mechanical properties of the SA-based films were investigated, and we found much improvement with MA addition and radiation dose. To produce efficient and cost-effective biocompatible food-packaging films, further investigations, such as biological testing, toxicity testing, and morphological analysis, are under consideration for the sustainable development of the SA-based films.

ACKNOWLEDGMENTS

The authors acknowledge financial support received from International Atomic Energy Agency (IAEA) (contract grant number 17639).

REFERENCES

1. Krause, S. *Polymer Blends*; Academic: New York, **1978**; Vol. 1, p 15.
2. Varnell, D. F.; Coleman, M. M. *Polymer* **1981**, *22*, 1324.
3. Varnell, D. F.; Runt, J. P.; Coleman, M. M. *Polymer* **1983**, *24*, 37.
4. Woo, E. M.; Barlow, J. W.; Paul, D. R. *J. Appl. Polym. Sci.* **1986**, *32*, 3889.
5. Miya, M.; Iwamoto, R. *J. Polym. Sci. Polym. Phys. Ed.* **1984**, *22*, 1149.
6. Patel, G. M.; Patel, C. P.; Trivedi, H. C. *Eur. Polym. J.* **1999**, *35*, 201.
7. Yang, J.; Wang, N.; Chiu, H. J. *Membr. Sci.* **2014**, *457*, 139.

8. Woods, R. T.; Pikaev, A. K. *Applied Radiation Chemistry: Radiation Processing*; Wiley: New York, **1994**.
9. Rahman, M. W.; Haque, M. E.; Rahman, M. M.; Abedin, M. *Z. Polym. Plast. Technol. Eng.* **2009**, *48*, 696.
10. Rahman, M. W.; Hossain, M. M.; Alam, M. J.; Dafader, N. C.; Haque, M. E. *Int. J. Polym. Anal. Chem.* **2013**, *18*, 479.
11. Schmid, M.; Held, J.; Hammann, F.; Schlemmer, D.; Noller, K. *Packag. Technol. Sci.* **2015**, *28*, 883.
12. Ghoshal, S.; Khan, M. A.; Noor, F. G.; Khan, R. A. *J. Macromol. Sci. Pure Appl. Chem.* **2009**, *46*, 975.
13. Choi, W. S.; Ahn, K. J.; Lee, D. W.; Byun, M. W.; Park, H. J. *Polym. Degrad. Stab.* **2002**, *78*, 533.
14. Cho, M.; Kim, B. Y.; Rhim, J. H. *Food Eng. Prog.* **2003**, *7*, 141.
15. Kang, H. J.; Jo, C.; Lee, N. Y.; Kwon, J. H.; Byun, M. W. *Carbohydr. Polym.* **2005**, *60*, 547.
16. Brault, D.; D'Aprano, G.; Lacroix, M. *J. Agric. Food Chem.* **1997**, *45*, 2964.
17. Jo, C.; Kang, H. J.; Lee, N. Y.; Kwon, J. H.; Byun, M. W. *Radiat. Phys. Chem.* **2005**, *72*, 745.
18. Hirano, S.; Mizutani, C.; Yamaguchi, K.; Miura, O. *J. Biopolym.* **1978**, *17*, 805.
19. Bailey, F. E. J.; Koleske, J. V. *Poly(ethylene oxide)*; Academic: New York, **1976**.
20. Osuna, I. B.; Ferrero, C.; Castellanos, M. R. *J. Eur. J. Pharm. Biopharm.* **2005**, *59*, 537.
21. Shah, S. B.; Patel, C. P.; Trivedi, H. C. *Carbohydr. Polym.* **1995**, *26*, 61.
22. Hendrix, K. M.; Morra, M. J.; Lee, H. B.; Min, S. C. *Food Hydrocolloids* **2012**, *26*, 118.
23. The, D. P.; Peroval, C.; Debeaufort, F.; Despre, D.; Courthaudon, J. L.; Voilley, A. *J. Agric. Food Chem.* **2002**, *50*, 2423.
24. McHugh, T. H.; Avena-Bustillos, R.; Krochta, J. M. *J. Food Sci.* **1993**, *58*, 899.
25. Standard Test Method for Water Vapor Transmission of Materials; ASTM E96-90. Annual Book of American Standards Testing Methods Standard; American Society for Testing and Materials: Philadelphia, PA, **1990**; p 834.
26. Caykara, T.; Demirci, S.; Eroglu, M. S.; Guven, O. *Polymer* **2005**, *46*, 10750.
27. Liang, C. X.; Hirabayashi, K. *J. Appl. Polym. Sci.* **1992**, *45*, 1937.
28. Xiao, C.; Lu, Y.; Liu, H.; Zhang, L. *J. Macromol. Sci. Pure Appl. Chem.* **2000**, *37*, 1663.
29. Gontard, N.; Guilbert, S.; Cuq, J. L. *J. Food Sci.* **1993**, *58*, 206.
30. Sothornvit, R.; Krochta, J. M. *J. Agric. Food Chem.* **2000**, *48*, 6298.
31. Rodriguez, M.; Oses, J.; Ziani, K.; Mate, J. I. *Food Res. Int.* **2006**, *39*, 840.
32. Yang, L.; Paulson, A. T. *Food Res. Int.* **2000**, *33*, 563.
33. Donhowe, G.; Fennema, O. *J. Food Process. Pres.* **1993**, *17*, 247.
34. Tuhin, M. O.; Rahman, N.; Haque, M. E.; Khan, R. A.; Dafader, N. C.; Islam, R.; Nurnabi, M.; Tonny, W. *Radiat. Phys. Chem.* **2012**, *81*, 1659.
35. Zelinska, K.; Shostenko, A. G.; Truszkowski, S. *High Energy Chem.* **2009**, *43*, 445.
36. Alam, R.; Khan, M. A.; Khan, R. A.; Ghoshal, S.; Mondal, M. I. H. *J. Polym. Environ.* **2008**, *16*, 213.
37. Nunthanid, J.; Puttipipatkachorn, S.; Yamamoto, K.; Peck, G. E. *Drug Dev. Ind. Pharm.* **2001**, *27*, 143.
38. Hoagland, P. D.; Parris, N. *J. Agric. Food Chem.* **1996**, *44*, 1915.
39. Kamper, S. L.; Fennema, O. *J. Food Sci.* **1984**, *49*, 1478.
40. Mollah, M. Z. I.; Khan, A. M.; Khan, A. R. *Radiat. Phys. Chem.* **2009**, *78*, 61.
41. Dangaran, K. L.; Cooke, P.; Tomasula, P. M. *J. Food Sci.* **2006**, *71*, 196.
42. Kumar, S.; Jog, J. P.; Natarajan, U. *J. Appl. Polym. Sci.* **2003**, *89*, 1186.
43. Yang, J. M.; Chiu, H. C. *J. Membr. Sci.* **2012**, *419*, 65.
44. Soares, J. P.; Santos, J. E.; Chierice, G. O.; Cavaleiro, E. T. G. *Eclética Quím.* **2004**, *29*, 57.
45. Pinhas, M. D.; Peled, H. B. *Acta Biomater.* **2011**, *7*, 2817.
46. Lee, Y. M.; Kim, S. S.; Kim, S. H. *J. Mater. Sci. Mater. Med.* **1997**, *8*, 537.
47. Moon, S.; Ryu, B. Y.; Choi, J.; Jo, B.; Farris, R. *J. Polym. Eng. Sci.* **2009**, *49*, 52.
48. Laurienzo, P.; Malinconico, M.; Motta, A.; Vicinanza, A. *Carbohydr. Polym.* **2005**, *62*, 274.
49. Bradley, S. A.; Carr, S. H. *J. Polym. Sci. Polym. Phys. Ed.* **1976**, *14*, 111.
50. Pizzoli, M.; Ceccorulli, G.; Scandola, M. *Carbohydr. Res.* **1991**, *222*, 205.
51. Ratto, J. A.; Chen, C. C.; Blumstein, R. B. *J. Appl. Polym. Sci.* **1996**, *59*, 1451.
52. Roger, S.; Bee, A.; Balnois, E.; Bourmaud, A.; Deit, L. H.; Grohens, Y.; Cabuil, V. Presented at the Fifth International Conference on Polymer–Solvent Complexes and Intercalates, Lorient, France, **2004**.
53. Mutalik, V.; Manjeshwar, L. S.; Wali, A.; Sairam, M.; Raju, K. V. S. N.; Aminabhavi, T. M. *Carbohydr. Polym.* **2006**, *65*, 9.
54. Knight, W. J. M.; Karasz, F. E.; Fried, J. R. *Solid State Transition Behavior of Blends*; Academic: New York, **1978**; p 185.
55. Olabishi, O.; Robeson, L. M.; Shaw, M. P. *Methods for Determining Polymer–Polymer Miscibility*; Academic: New York: **1979**.
56. Wang, W.; Wang, A. *Carbohydr. Polym.* **2010**, *80*, 1028.
57. Mandal, B.; Ray, S. K. *Carbohydr. Polym.* **2013**, *98*, 257.
58. Yadav, M.; Rhee, K. Y. *Carbohydr. Polym.* **2012**, *90*, 165.